Zheng, Jianfang; Ala-Laurinaho, Juha; Sneck, Asko; Mäkelä, Tapio; Alastalo, Ari; Räisänen, Antti

Roll-to-roll reverse offset printing of millimeter-wave transmission lines and antennas on flexible substrates

Published in:
12th European Conference on Antennas and Propagation (EuCAP 2018)

DOI:
10.1049/cp.2018.0443

Published: 10/12/2018

Document Version
Peer reviewed version

Please cite the original version:
Zheng, J., Ala-Laurinaho, J., Sneck, A., Mäkelä, T., Alastalo, A., & Räisänen, A. V. (2018). Roll-to-roll reverse offset printing of millimeter-wave transmission lines and antennas on flexible substrates. In 12th European Conference on Antennas and Propagation (EuCAP 2018) https://doi.org/10.1049/cp.2018.0443

Roll-to-Roll Reverse Offset Printing of Millimeter-wave Transmission Lines and Antennas on Flexible Substrates

Jianfang Zheng[1], Juha Ala-Laurinaho[1], Asko Sneck[2], Tapio Mäkelä[2], Ari Alastalo[2], Antti V. Räisänen[1]
[1]Department of Electronics and Nanoengineering, Aalto University, Espoo, Finland, jianfang.zheng@aalto.fi
[2]VTT, Technical Research Centre of Finland

***Abstract*—We investigate the feasibility of roll-to-roll reverse offset (R2R-RO) printing technology for the mass fabrication of millimeter-wave antennas on flexible substrates. In this study, samples of coplanar waveguide (CPW) transmission lines and microstrip patch antennas were manufactured and measured. The results indicate that the R2R-RO printing technique can be an excellent candidate for the production of millimeter-wave and terahertz devices, since it has the advantage of low cost and high resolution.**

***Index Terms*—millimeter wave, roll-to-roll printing, flexible substrate, antenna, measurement.**

I. Introduction

Recently, the topics of Internet of Things (IoT) and the fifth generation (5G) have been becoming more and more popular. In order to meet the requirements of data traffic, millimeter-wave (mm-wave) technology has been recognized as a key technology in IoT and 5G communications systems. They need low-cost electronics with high performance and smaller dimensions. Mm-wave technology, however, has been too expensive to adapt it to consumer products.

Printed electronics has advantages in terms of weight, flexibility, and ease of integration into portable devices and several state-of-art achieved results have been summarized [1]–[4]. Many high-resolution printing methods have been proposed, but so far they are limited by the line resolution, materials, low speed, or insufficient aligning accuracy [5]–[7].

In this work, we aim at developing the roll-to-roll reverse offset (R2R-RO) technology to make the manufacturing process possible for millimeter-wave structures. Coplanar waveguide (CPW) transmission lines and microstrip patch antennas printed by R2R-RO printing technology have been investigated, fabricated, and measured.

II. CPW Transmission Lines

In the process of R2R-RO printing, the conductive ink is applied on a polydimethylsiloxane (PDMS) blanket wrapped around a cylinder. Stamp on another cylinder takes part of the ink away, whereas the remaining ink on the stamp forms the pattern on the substrate (Fig. 1) [8]. To ensure the flat conducting ink layer with even thickness in large printing areas, some pillar-shape structures are necessary for the manufacturing. These are shown as holes on the printed ink layer.

(a)

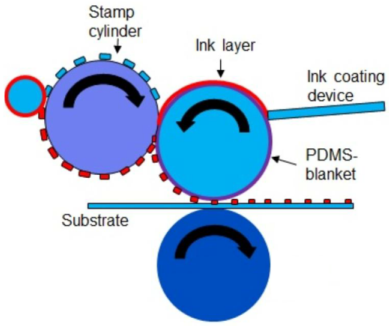

(b)

Fig. 1: (a) Print flow in R2R-RO printing, from left to right. (b) Process diagram of R2R-RO method in this research.

The substrates used in our printing experiments are Polyethylene Naphthalate (PEN) substrates with thickness of 125 µm and with measured dielectric constant ϵ_r = 3.2 and loss tangent tanδ = 0.045 at 90 GHz [9]. The printed silver nanoparticle ink is sintered producing metal layers resistivity of $\rho \approx 2.5 \times 10^{-7}$ Ω·m or conductivity of $\sigma \approx 4 \times 10^{6}$ S/m. When taking into account the sintered ink layer thickness of 300 - 400 nm, we use the sheet impedance of square impedance ≤ 1 Ω/sq, representing the ability of ink to conduct electricity.

A. CPW Design

CPW is used widely as a transmission line in mm-wave frequency band structures, and it is the simplest structure for measuring in the probe station environment. Therefore, we investigate the CPW transmission lines with holes on the conductor layer applicable for the R2R-RO printing technology in the frequency range of 67-110 GHz which covers the full W-band (75-110 GHz).

The dimensions of CPW we choose for the 50 Ω characteristic impedance on the PEN substrate (h = 125 µm, ϵ_r = 3.2) are: signal line width w_{cpw} = 150 µm and gap width w_{gap} = 13 µm. With the holes on the metal layer, the physical structure of the CPW will be changed, so we need to optimize the parameters of the holes to keep the CPW performance stable. Depending on different printing directions (x and y), we put periodical holes in the metal layer. The radius of the holes is r = 10 µm, and the distances between the holes in two orthogonal directions are 60 µm and 100 µm (Fig. 2). To reduce the effect on surface currents on the CPW signal line edge, we removed some holes in Fig. 2(d) (reduced holes). Since the the conductivity of ink is not as good as that of the perfect electric conductor (PEC), we set the square impedance of conducting ink to R = 1 Ω/sq as a reference.

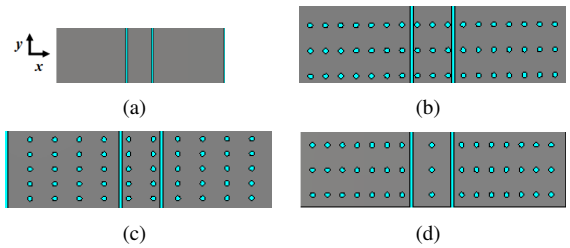

Fig. 2: (a) CPW full covered with metal (no holes); (b) with holes *dx*=60 µm, *dy*=100 µm; (c) with holes *dx*=100 µm, *dy*=60 µm; (d) holes *dx*=60 µm, *dy*=100 µm (with reduced holes).

A set of 2-mm-long CPW transmission lines (with and without holes) were designed with square impedance R = 1 Ω/sq. The simulated results of S-parameters are shown in Fig. 3. Since the CPW transmission lines are symmetric 2-ports passive devices, only results from port 1 are plotted. The reflection coefficient S_{11} in all cases is below -20 dB in the full frequency range. The transmission coefficient S_{21} for the case of CPW with holes in the metal layer is a bit lower than that of when it is fully covered with conducting ink, because the hole structure affects the surface current distribution on the CPW signal line and increases the equivalent sheet impedance. Thus, the more holes on the CPW signal line (dx = 60 µm, dy = 100 µm in Fig. 2(b)), the worse the sheet impedance becomes (yellow dot line in Fig. 3).

B. CPW Measurement

Microscope views of the fabricated CPW transmission lines under the probe station measurement environment are shown in Fig. 4. The holes are periodically located along the two orthogonal edges. The overall manufacturing quality of R2R-RO printing is very excellent, which can reach a resolution of $\leq$10 µm.

We measured the CPW transmission lines with on-wafer ground-signal-ground (GSG) probes. The measured results of two chosen CPW samples are shown in Fig. 5. It is clear that the reflection coefficients S_{11} are less than -15 dB in the full frequency range. The level of the transmission coefficients S_{21} is a little higher than the simulated one, which indicates that the practical conducting ink has a sheet impedance less than 1 Ω/sq. Another reason could be that the actual loss tangent of

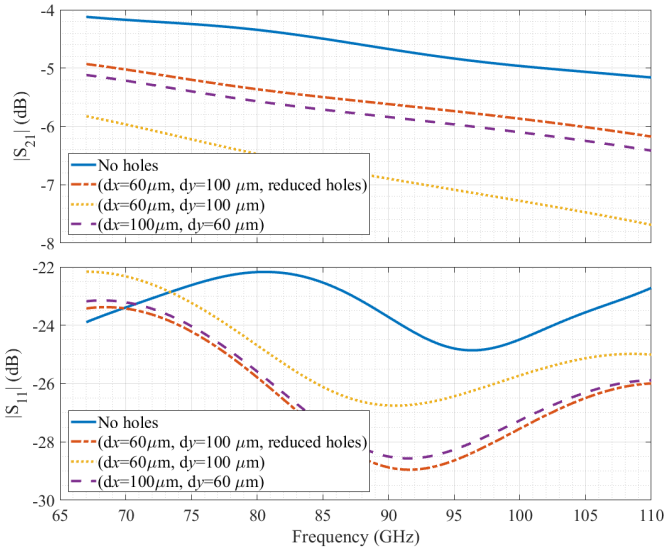

Fig. 3: S-parameter simulation results of different type of CPW transmission lines with ink sheet impedance R= 1 Ω/sq. The length is 2 mm.

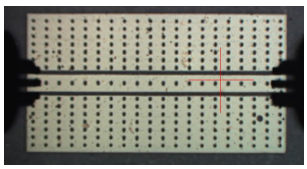

(a) (b)

Fig. 4: Microscope views of fabricated printed CPW transmission lines fed with GSG probes. (a) *dx*=100 µm, *dy*=60 µm; (b) *dx*=60 µm, *dy*=100 µm (with reduced holes). The length is 2 mm.

PEN substrates is lower than the measured value in [9]. It is worth mentioning that the measured S_{21} parameters show the same trend as simulated results, i.e. that less holes on CPW signal line will result in less losses.

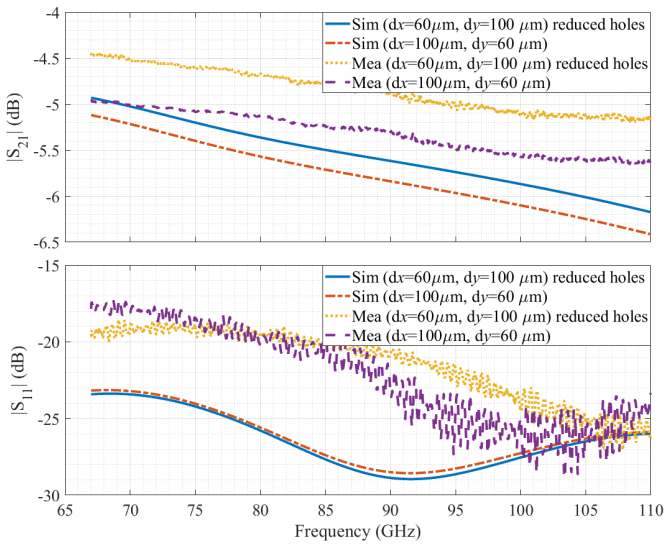

Fig. 5: S-parameter measurement results of CPW transmission lines. The length is 2 mm.

III. Microstrip Patch Antennas

We have also investigated the feasibility of R2R-RO printing technology on printing large-area structures, i.e. microstrip patch antenna, patch array, and grid antennas. In this paper, a printed microstrip patch antenna is presented.

A. Design and Fabrication

In Section II, we have discussed CPW-type transmission lines. The CPW is also used as the starting part of the feeding structure in the microstrip patch antenna, because in the mm-wave frequency, it is difficult to feed antennas by coaxial lines due to the limited antenna size. We designed a microstrip patch antenna working in the center frequency of 77 GHz. Some basic parameters of the antenna in this design are: the 50 Ω microstrip line width w_{ms} = 0.28 mm, sizes of patch l_{patch} = 1.8 mm and w_{patch} = 1 mm (Fig. 6(a)). Like CPW transmission lines, the same periodically situated holes are also added in the metal layer.

A microscope view of printed microstrip patch antenna is depicted in Fig. 6(b). It is clearly seen that the antenna has been printed with a very good dimensional quality.

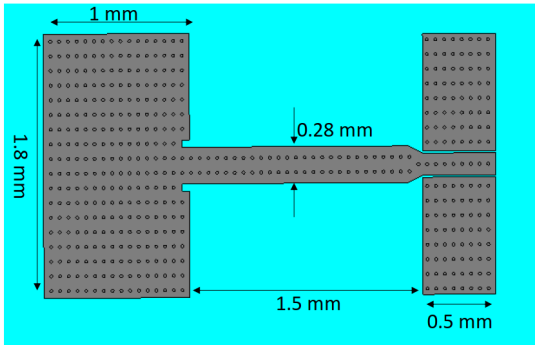

(a)

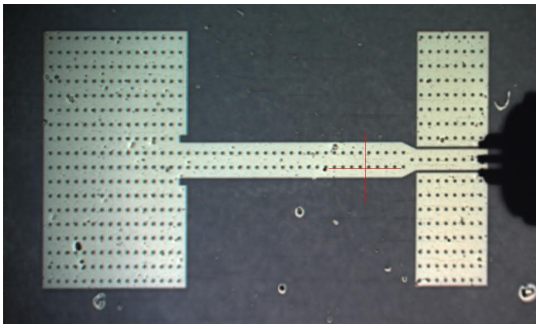

(b)

Fig. 6: (a) Dimensions of the designed patch antenna; (b) Microscope view of a fabricated printed microstrip patch antenna with GSG feeding probe.

B. Simulation and Measurement Results and Analysis

Similarly to CPW transmission line measurements, we measured the microstrip patch antenna on the on-wafer probe station in the frequency range of 67-110 GHz. Both the reflection coefficient S_{11} and the realized gain were measured.

1) Reflection Coefficient Measurement: The simulated reflection coefficient S_{11} of the designed antenna is presented by the blue dash line in Fig. 7, and it has the first resonance frequency of 77 GHz. The measured S_{11} is shown as the yellow solid line in Fig. 7, which has the first resonance frequency of 81 GHz. There is a frequency shift between the simulated and measured results. Possible reason for this is explained later.

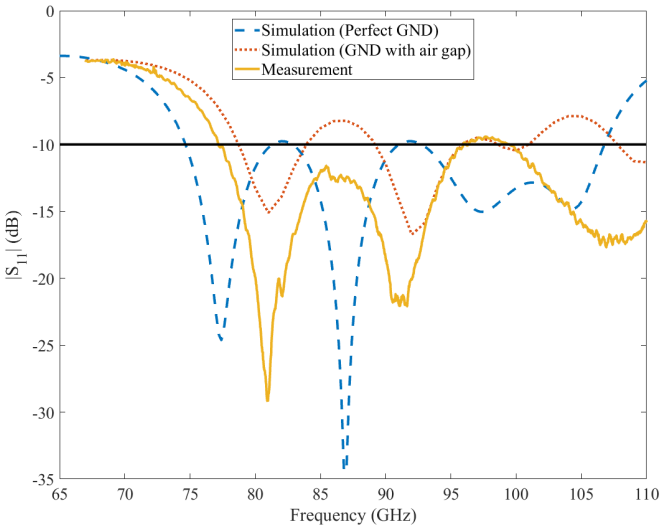

Fig. 7: Simulated and measured reflection coefficients of the microstrip patch antenna.

2) Realized Gain Measurement: Due to the limitation of the set-up in the probe station, we can not measure the antenna radiation pattern with a rotator. Alternatively, we only measured the maximum realized gain in the broadside diection, i.e. in the angle ($\theta = 0°, \phi = 0°$), where the main beam of the designed microstrip patch antenna is pointing at. The method we used for the gain measurement is presented in [10].

The simulated realized gain-frequency curve is the blue dash line in Fig. 8. The realized gain peaks at a little higher frequency than the designed resonance frequency 77 GHz. The simulated realized gain value is 4.5 dBi at 77 GHz, whereas it peaks at 79 GHz with level of 4.8 dBi. The measured realized gain-frequency curve is shown in Fig. 8 (yellow solid line). It is clear that compared with the simulated gain curve, the measured realized gain has a frequency shift leading to a good radiation at the resonance frequency of about 81 GHz and the peak value is 4.5 dBi at 84 GHz.

3) Analysis of Measured Realized Gain: In Section III-B1 and Section III-B2, we observe that there is a frequency shift between simulated and measured results for the microstrip patch antenna. The structural dimensions of the fabricated samples are measured and they follow very accurately the designed values. Also, the thickness of the substrate was measured and it is close to nominal 125 µm within few micrometer accuracy. According to the simulation, the small discrepancy in thickness has negligible effect on the performance of the antenna. Therefore, dimensional inaccuracies are not seen as the reason for the frequency shift. In addition, we

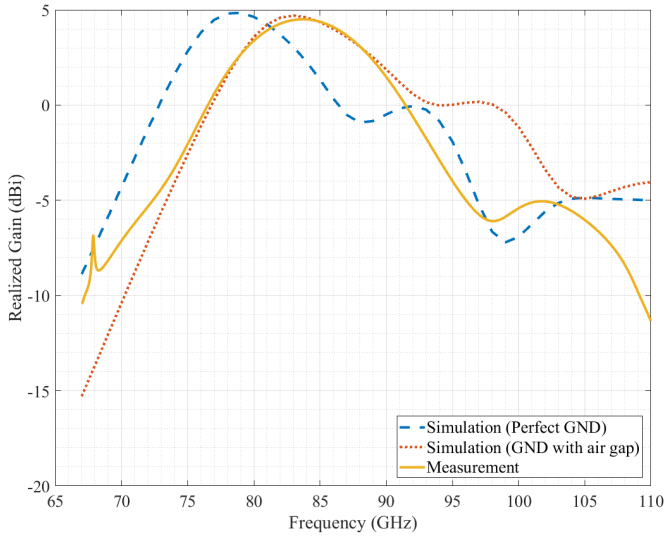

Fig. 8: Simulated and measured realized gains of the microstrip patch antenna.

have estimated how the change in the substrate permittivity affects the resonance frequency. The simulation shows the observed resonance frequency corresponds to the substrate permittivity of 2.8. We have made further measurement for the material parameters, verifying the dielectric constant of the PEN substrate is 3.2 with an accuracy of 0.1.

Instead of discrepancy in material properties or dimensions, we suspect the measurement environment to be the cause of the frequency shift. The designed antenna has a perfect ground (GND), but the fabricated sample does not have a GND on the back side, and we use the steel chuck of the probe station as the GND. In this situation, there could be a small air gap between the metal surface and the bottom of the PEN substrate. To analyze quantitatively, we have done simulations and varied the air gap. The measured and simulation results agree best when the air gap is 12 µm. The simulated S_{11} and realized gain curves are shown as the red dot lines in Fig. 7 and Fig. 8. In this case, the measured results match the simulated results excellently.

IV. Conclusion and Future Work

CPW transmission lines and microstrip patch antennas based on R2R-RO printing technology have been designed, fabricated, and measured. The process is cost-effective with excellent resolution and can be suitable for large-area printing. The performances of the designed CPW and antennas satisfy the expectations. For example, the printed patch antenna has a measured peak realized gain of 4.5 dBi. R2R-RO printing technology is a good candidate for the fabrication of IoT and 5G devices.

Future work is still needed: e.g., to improve ink conductivity and fabricate metal GND layer on the back side of substrates to ensure good quality ground plane for the patch antenna.

Acknowledgment

The authors would like to thank Xuchen Wang for discussions and Mikko Heino for his help in the development of antenna measurement system.

This work is supported by Academy of Finland project #288145 (LATERA) and partly by Chinese Scholarship Council (CSC).

References

[1] F.C. Krebs, "Fabrication and processing of polymer solar cells: A review of printing and coating techniques", *Solar Energy Materials & Solar Cells*, vol. 93, no. 4, pp. 394-412, April 2009.

[2] W. Clemens, W. Fix, J. Ficker, A. Knobloch, A. Ullmann, "From polymer transistors toward printed electronics", *Journal of Materials, Research*, vol. 19, no. 7, pp. 1963-1973, 2004.

[3] J. Zheng, J. Ala-Laurinaho, A. Alastalo, T. Mäkelä, A. Sneck, and A. V. Räisänen, "Studies on applicability of reverse offset in printing mm-wave antennas on flexible substrates," *2017 10th Global Symposium on Millimeter-Waves*, Hong Kong, 2017, pp. 42-43.

[4] A. V. Räisänen, J. Ala-Laurinaho, V. Asadchy, A. Diaz-Rubio, S. Khanal, V. Semkin, S. Tretyakov, X. Wang, J. Zheng, A. Alastalo, T. Mäkelä, and A. Sneck, " Suitability of roll-to-roll reverse offset printing for mass production of mm-wave antennas: Progress report," *2016 Loughborough Antennas & Propagation Conference (LAPC)*, Loughborough, 2016.

[5] P.F. Moonen, I. Yakimets, and J. Huskens, "Fabrication of transistors on flexible substrates, from mass-printing to high-resolution alternative lithography strategies," *Advanced Materials*, vol. 24, no. 41, pp. 5526-5541, 2012.

[6] S. Khan, L. Lorenzelli, and R.S. Dahiya, "Technologies for printing sensors and electronics over large flexible substrates: a review," *IEEE Sensors Journal*, vol. 15, no. 6, pp. 3164-3184, June 2015.

[7] M. Koutake and Y. Katayama, "Reverse offset printing and specialized inks for organic TFTs," *Int. Conf. on Electronics Packaging (ICEP2014)*, Toyama, Apr. 2014, pp. 279-282.

[8] A. Alastalo, A. Sneck and T. Mäkelä, "Towards roll-to-roll reverse-offset printing," *9th International Exhibition and Conference for the Printed Electronics Industry (LOPEC)*, München, March, 2017.

[9] S. Khanal, V. Semkin, V. Asadch, J. Ala-Laurinaho, A. Alastalo, A. Sneck, T. Mäkelä, S. Tretyakov, and A. V. Räisänen, "Towards printed millimeter-wave components: Material characterization," *2016 Global Symposium on Millimeter Waves (GSMM) & ESA Workshop on Millimetre-Wave Technology and Applications*, Espoo, 2016.

[10] J. Zheng, J. Ala-Laurinaho, and A. V. Räisänen, "A simple method for on-wafer antenna gain measurement," *The 38th Progress In Electromagnetics Research Symposium*, St. Petersburg, 2017.